

**ANALYSIS OF CRISM AND OMEGA OBSERVATIONS OF PHOBOS AND DEIMOS.** A. A. Fraeman<sup>1</sup>, R. E. Arvidson<sup>1</sup>, S. L. Murchie<sup>2</sup>, A. S. Rivkin<sup>2</sup>, J-P Bibring<sup>3</sup>, B. Gondet<sup>3</sup>, N. Manaud<sup>4</sup>, Y. Langevin<sup>3</sup>, T. Choo<sup>2</sup>, D. Humm<sup>2</sup> <sup>1</sup>Washington University in St. Louis (afraeman@wustl.edu), <sup>2</sup>Johns Hopkins Applied Physics Laboratory, <sup>3</sup>Institut d'Astrophysique Spatiale, <sup>4</sup>European Space Astronomy Centre, Madrid, Spain

**Introduction:** The Compact Reconnaissance Imaging Spectrometer for Mars (CRISM) and the Observatoire pour la Mineralogie, l'Eau, les Glaces et l'Activité (OMEGA) have both acquired disk-resolved, visible to near infrared hyperspectral images Phobos, and Deimos has been observed by CRISM. Data from these two instruments provide the highest spatial resolution spectra of Phobos ever acquired, as well as the first disk-resolved hyperspectral observation of Deimos. Here we discuss these data and analyze them for clues to Phobos' and Deimos' surface compositions.

**Data sets:** In its high-resolution targeted mode, CRISM acquires spectra in 544 wavelengths from 0.4  $\mu\text{m}$  to 3.92  $\mu\text{m}$  [1]. The CRISM data consist of three Phobos observations acquired in succession on 23 October 2007. They each have an average phase angle of 41°, spatial resolution of 350 m/pixel, and cover approximately the same spatial region in the western side of Phobos' sub-Mars hemisphere. The three Deimos observations were acquired in June 2007, and are the first hyperspectral data that spatially resolve the disk of Deimos, having spatial resolutions of 1.2 km/pixel. Similar to the Phobos data, the three Deimos observations were collected sequentially and provide overlapping coverage of the sub-Martian hemisphere of Deimos at an average phase angle of 22°.

OMEGA covers to longer wavelengths but has lower spectral resolution, observing from 0.38  $\mu\text{m}$  to 5.1  $\mu\text{m}$  in 352 spectral channels [2]. OMEGA acquired ten separate observations of Phobos between May 2004 and January 2011. We focus on six of the ten observations that contain the highest quality data from OMEGA's full wavelength range of 0.38  $\mu\text{m}$  to 5.1  $\mu\text{m}$ . These data provide phase angle coverage from 38° to 99°, spatial resolutions from 120 m/pixel to 2200 m/pixel, and broad coverage of both the sub- and anti-Mars hemispheres of Phobos.

The incidence ( $i$ ), emergence ( $e$ ), and phase angles ( $\alpha$ ) for each pixel in the CRISM observations were determined using the shape model of Thomas and the SciBox Toolkit developed at the Johns Hopkins Applied Physics Laboratory [3,4]. The photometric angles for the OMEGA data were computed using a prototype version of the Navigation and Ancillary Information Facility (NAIF) SPICE Toolkit that includes a Digital Shape Kernel (DSK) system in conjunction with a Phobos DSK model.

**Photometric Analysis:** The broad phase angle coverage of the six OMEGA observations allows us to use these data to derive wavelength dependent photometric parameters from 0.4 to 2.5  $\mu\text{m}$ . Here, re-

flected solar radiance is the dominant component of spectra and may be modeled using Hapke's equation for radiance factor ( $r$ ):

$$r(i, e, \alpha) = \frac{w - \mu_0}{4\pi \mu_0 + \mu} [(1 + B(\alpha))p(g_1) + H(w, \mu_0)H(w, \mu) - 1] \cdot S(i, e, \alpha, \theta)$$

where  $w$  is the average single scattering albedo,  $\mu$  and  $\mu_0$  are the cosines of  $e$  and  $i$  angles respectively,  $B(\alpha)$  models the opposition-effect,  $p(g_1)$  is the 1-term Henyey-Greenstein phase function with asymmetry factor  $g_1$ ,  $H$  is an approximation for the isotropic multiple scattering function, and  $S(\theta)$  is a function related to surface roughness [5].

We searched for the values of  $w$ ,  $g_1$ , and  $\theta$  that would provide the best global average fit for the surface of Phobos. Fig. 1 shows the wavelength-dependent, global average best-fit values for  $w$  and  $g_1$  at selected wavelengths with  $\theta = 14^\circ$ , which is the average best fit value for  $\theta$  at all wavelengths. We find that  $w$  increases monotonically while  $g_1$  is essentially constant with wavelength and indicative of a mildly backscattering surface. The 1- $\sigma$  uncertainties on  $w$  are much smaller than the 1- $\sigma$  uncertainties of  $g_1$ , consistent with range and distribution of phase angles covered by the six OMEGA observations [6]

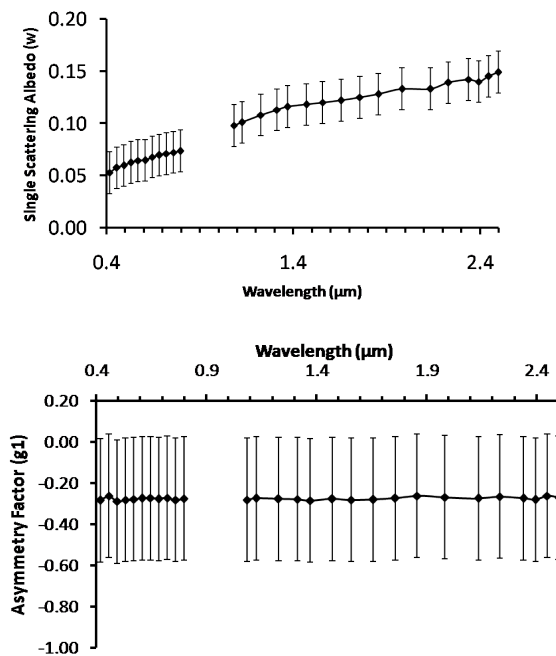


Figure 1: Best fit single scattering albedo (top) and asymmetry parameter (bottom) as a function of wavelength assuming wavelength independent values of  $\theta = 14^\circ$ ,  $B_0 = 5.702$ ,  $h = 0.072$ . Values for  $B_0$  and  $h$  from [7].

Thermal emission becomes significant at wavelengths longer than  $2.5 \mu\text{m}$  and must be modeled together with reflected light contributions. The Hapke model is modified to take into account the addition of a directional-hemispherical thermal emission component assuming a given temperature. Not only does the addition of a thermal emission component introduce another unknown to the model in the form of temperature, but it also makes it more challenging to solve for global average parameters because temperature varies from pixel to pixel. We have used a variety of techniques to solve for  $w$  in this region, and are confident of retrieved spectra out to  $\sim 4 \mu\text{m}$ .

**Spectral analysis:** Phobos spectra are photometrically corrected by assuming  $g_l = -0.3$  and  $\theta = 14^\circ$  at all wavelengths and solving for the wavelength-dependent single scattering albedo,  $w$ . The  $0.5 - 1.0 \mu\text{m}$  slope differences between the region east of Stickney versus the "average" Phobos unit are consistent with the finding that Phobos contains at least two distinct spectral units distinguished on the basis of spectral slope [8].

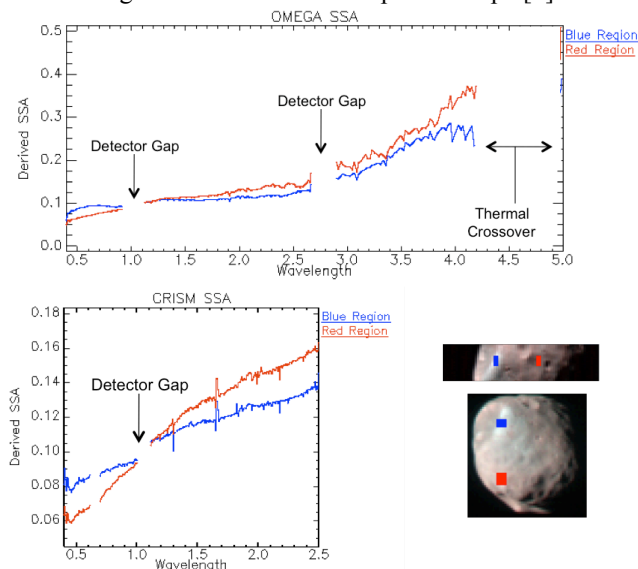


Fig 2: Average single scattering albedo spectra from different spectral units on Phobos from OMEGA (top) and CRISM (bottom) data.

**Feature around  $0.65 \mu\text{m}$ :** Initial analyses of the CRISM Phobos and Deimos observations revealed the presence of a broad, shallow feature centered around  $0.65 \mu\text{m}$  and associated only with the redder spectral unit on Phobos [9]. The  $0.65 \mu\text{m}$  feature also appears in photometrically corrected single scattering albedo spectra from CRISM. Figure 3 shows the  $0.6 \mu\text{m}$  band depth map created from CRISM and OMEGA observations covering the sub-Martian hemisphere of Phobos. The CRISM Deimos observations also show the presence of a  $0.65 \mu\text{m}$  feature in every pixel of the observation (Fig. 3).

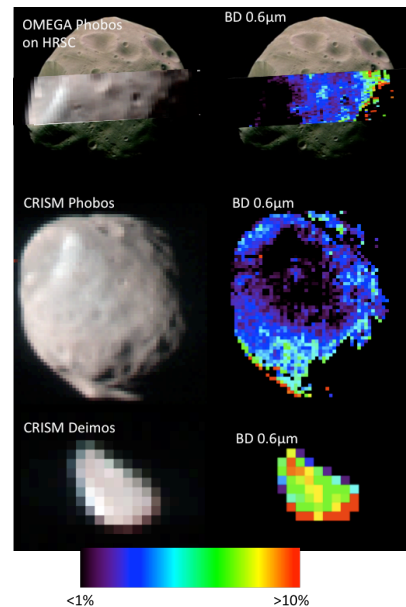


Fig 3:  $0.6 \mu\text{m}$  band depth maps for OMEGA (top) and CRISM (middle) data of Phobos, and CRISM data of Deimos (bottom).

**Search for mafic absorptions:** We have searched for mafic mineral features in the CRISM and OMEGA dataset by generating mafic mineral summary parameter maps commonly used in analysis of CRISM and OMEGA observations. We specifically examined summary parameters designed to highlight the presence of olivine and low- and high-calcium pyroxene. The resulting maps generated from the photometrically corrected Phobos and I/F Deimos observation show little or no indication for any of these minerals, and we conclude that there is no evidence for mafic mineral absorption features above the level of instrument noise.

**Discussion:** Broad and shallow spectral features centered between  $0.6 - 0.8 \mu\text{m}$  very similar to those in the Phobos and Deimos spectra are frequently observed in low albedo asteroids (C- D- and P-class) and carbonaceous chondrites [10,11]. While the cause of these absorptions is commonly attributed to phyllosilicates with  $\text{Fe}^{2+}/\text{Fe}^{3+}$  charge transfer, it is unclear whether phyllosilicates are the source of the  $0.65 \mu\text{m}$  feature observed on Phobos and Deimos metal-OH absorptions diagnostic of phyllosilicates have not been observed in the moons' spectra. We are therefore considering additional interpretations at present.

**References:** [1] Murchie, S. et al. (2007) 112, E05S03. [2] Bibring, J-P. et al. (2004) *Mars Express: The Scientific Payload*, 37-49. [3] Thomas, P. (1993) *Icarus*, 205, 326-344. [4] Choos, T & Skura, J. (2004) *Johns Hopkins APL Technical Digest*, 25, 154-162. [5] Hapke, B. (1993) *Theory of Reflectance and Emittance Spectroscopy*. [6] Helfenstein, P. & Veeverka, J. (1989) *Asteroids II*, 557-593. [7] Simonelli, D. et al. (1998) *Icarus*, 131, 53-77. [8] Murchie, S. and Erard, S. (1996) *Icarus*, 123, 63-86. [9] Murchie, S. et al. (2008) *LPS XXXIX*, 1434. [10] Cloutis, E. et al., (2011) *Icarus*, 212, 180-209. [11] Cloutis, E. et al., (2011) *Icarus*, 216, 309-349.